DALTON
FULL PAPER

Complex-formation reactions of Cu(II) and Zn(II) 2,2′-bipyridine and 1,10-phenanthroline complexes with bicarbonate. Identification of different carbonate coordination modes

Zong-Wan Mao,[a,b] Frank W. Heinemann,[a] Günther Liehr[a] and Rudi van Eldik *[a]

[a] *Institute for Inorganic Chemistry, University of Erlangen-Nürnberg, Egerlandstr. 1, 91058 Erlangen, Germany. E-mail: vaneldik@chemie.uni-erlangen.de*
[b] *School of Chemistry and Chemical Engineering, Zhongshan University, 510275 Guangzhou, P. R. China*

Received 2nd May 2001, Accepted 15th October 2001
First published as an Advance Article on the web 27th November 2001

A series of carbonato complexes was isolated in the reaction of $[ML_2(H_2O)]^{2+}$ (M = Cu(II), Zn(II), L = bpy (2,2′-bipyridyl) and phen (1,10-phenanthroline) with HCO_3^-. Two monomeric carbonato Cu(II) complexes with different bidentate distortion, $[Cu(phen)_2(CO_3)]\cdot 7H_2O$ and $[Cu(phen)_2(CO_3)]\cdot 11H_2O$, and three binuclear carbonato complexes with four different bridging modes, $\{[Cu(phen)_2]_2(\mu_2\text{-}CO_3)\}(ClO_4)_2\cdot 4.25H_2O$ containing two different carbonate coordination modes, $\{[Cu(phen)_2]_2(\mu_2\text{-}CO_3)\}(ClO_4)_2\cdot DMF\cdot H_2O$ and $[(bpy)_2(H_2O)Zn(\mu_2\text{-}CO_3)Zn(bpy)_2](NO_3)_2\cdot 7H_2O$, were characterized by X-ray crystallography. UV-Vis spectra of $[CuL_2(H_2O)]^{2+}$ ions were recorded as a function of pH in the absence and presence of $NaHCO_3$, and revealed evidence for a carbonation process in the pH range 6 to 10 and a hydrolysis process in the pH range 10 to 13. ^{13}C NMR spectra of $[(bpy)_2(H_2O)Zn(\mu_2\text{-}CO_3)Zn(bpy)_2]^{2+}$ revealed formation of polynuclear carbonato complexes in solution. Complex-formation kinetics of $[CuL_2(H_2O)]^{2+}$ (L = bpy and phen) with HCO_3^- were studied by stopped-flow using a pH-jump technique. The results indicated rapid formation of $[Cu(bpy)_2OCO_2H]^+$ and $[Cu(phen)_2OCO_2H]^+$, followed by a slow step (induced by the pH jump) for which the observed first order rate constants were found to be identical for both complexes and independent of the complex and carbonate concentrations employed. The thermal and pressure activation parameters for this step were also determined. The reaction is assigned to a pH-jump induced ring-closure reaction of the unstable five-coordinate monodentate bicarbonato intermediates, $[Cu(bpy)_2OCO_2H]^+$ and $[Cu(phen)_2OCO_2H]^+$, to form the pseudo-octahedral bidentate carbonato complexes $[Cu(bpy)_2O_2CO]$ and $[Cu(phen)_2O_2CO]$, respectively. A possible mechanism for the carbonation of CuN_4 complexes with an in-plane coordinated water molecule in a trigonal bipyramidal structure is proposed.

Introduction

A significant advance has been made in the understanding of the hydration of carbon dioxide and dehydration of bicarbonate catalyzed by carbonic anhydrase in recent years as a result of the application of model compounds.[1–15] It has been widely accepted that the $R_3Zn\text{-}OH$ form is the active species in the hydration and the $R_3Zn\text{-}H_2O$ form in the dehydration reactions. A reaction mechanism is shown in Scheme 1. However, detailed

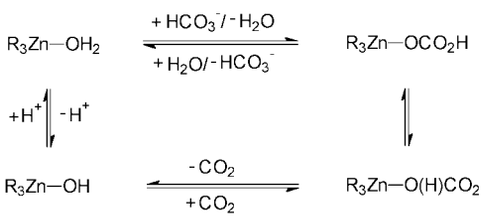

Scheme 1 The overall proposed catalytic mechanism for the carbonic anhydrase enzyme.

information on the binding mode of the bicarbonate intermediate in the catalytic cycle still remain unresolved, and for that reason studies on the interaction of bicarbonate with model Zn(II) and coloured metal complexes such as Cu(II), are of interest. The reaction of model compounds with CO_2/HCO_3^- produced, in specific cases, bicarbonate binding modes in monomers[16] and dimers.[17] So far, various carbonate bonding modes in monomers,[1i,18] dimers,[10,19] trimers,[13,20] tetramers,[21] hexamers[22] and 1D or 2D systems,[23] have been identified.

In our earlier work in this area, we studied the catalytic activity of carbonic anhydrase and model Zn(II) complexes in an indirect way employing an indicator method to monitor the pH changes associated with the hydration/dehydration processes.[11] In efforts to use an UV-Vis active metal center which will enable a direct monitoring of the catalytic process, we turned to model Cu(II) complexes. We first investigated the reactions of the Cu(II) complexes of 2,2′,2″-tris(2-aminoethyl)amine (tren) and tetraazacyclododecane ([12]aneN$_4$) with bicarbonate.[20i] It was found that $[Cu(tren)(H_2O)]^{2+}$ undergoes rapid substitution of H_2O by HCO_3^-, but no reaction occurred between $[Cu([12]aneN_4)(H_2O)]^{2+}$ and HCO_3^-. These results clearly demonstrate that the ability of $[CuN_4(H_2O)]^{2+}$ to react with HCO_3^- strongly depends on the position of the coordinated water molecule in the coordination sphere of the Cu(II) ion.

In order to study the relevance of the geometric configuration around the Cu(II) and Zn(II) centers for the catalytic activity of the enzyme during the dehydration process further, the present investigation focusses on Cu(II) and Zn(II) complexes with 2,2′-bipyridine (bpy) and 1,10-phenanthroline (phen) as spectator ligands,[24] in which a coordinated water molecule occupies the in-plane position of the trigonal bipyramidal structure. A completely different kinetic behavior was observed for these systems. We report a kinetic study of the reaction of $[Cu(bpy)_2(H_2O)]^{2+}$ and $[Cu(phen)_2(H_2O)]^{2+}$ with HCO_3^-, and the X-ray structures of five carbonato complexes

 DOI: 10.1039/b103942n

in which carbonate is bound as a monodentate and bidentate ligand to $Cu(phen)_2^{2+}$, or bridges two metal centers in a unique way in dimeric $Cu(phen)_2^{2+}$ and $Zn(bpy)_2^{2+}$ complexes. Plausible reaction mechanisms to account for the behavior of Cu(II) and Zn(II) carbonato complexes are proposed on the basis of the structural and kinetic information.

Experimental

Materials

All metal salts were of analytical reagent grade and used without further purification. 2,2′-Bipyridine and 1,10-phenanthroline were purchased from Aldrich. The complexes $[Cu(bpy)_2(H_2O)](NO_3)_2$ and $[Cu(phen)_2(H_2O)](NO_3)_2$ were prepared and characterized according to a literature method.[25] $NaHCO_3$ was obtained from Fluka and $NaH^{13}CO_3$ from Aldrich.

Syntheses

$[Cu(phen)_2(CO_3)]\cdot 7H_2O$ (1) and $[Cu(phen)_2(CO_3)]\cdot 11H_2O$ (2). A mixture of 0.283 g (0.5 mmol) of $[Cu(phen)_2(H_2O)](NO_3)_2$ and 0.336 g (4.0 mmol) of $NaHCO_3$ was dissolved in 20 mL of water and stirred for 5 min at room temperature. The solution was filtered and allowed to stand for slow evaporation in air. After a few days, a small amount of green crystals (**1**) and many blue block crystals (**2**) were obtained, suitable for X-ray analysis. The blue crystals (**2**) are unstable in air and soon change to green crystals (**1**). IR ν/cm^{-1} (KBr pressed pellet): 1332s for CO_3^{2-}. Anal. Calc. for $C_{25}H_{30}N_4O_{10}Cu$ (**1**): C, 49.22; H, 4.96; N, 9.18. Found: C, 49.56; H, 4.79; N, 9.02%.

$\{[Cu(phen)_2]_2(\mu_2\text{-}CO_3)\}(ClO_4)_2\cdot 4.25H_2O$ (3). A mixture of 0.258 g (0.5 mmol) of $[Cu(phen)_2(H_2O)](NO_3)_2$ and 0.084 g (1.0 mmol) of $NaHCO_3$ were dissolved in 20 mL of water and stirred for 5 min at room temperature. A saturated $NaClO_4$ solution was added dropwise and 0.251 g (39.7%) of blue powder crystals were immediately isolated through filtering. These crystals can also be obtained directly by the reaction of $[Cu(phen)_2(H_2O)](ClO_4)_2$ (obtained by addition of saturated $NaClO_4$ to a solution of the nitrate salt) with $NaHCO_3$. The crystals were recrystallized in aqueous solution and green-blue crystals were obtained, suitable for X-ray analysis. IR ν/cm^{-1} (KBr pressed pellet): 1359m for CO_3^{2-}, and 1089s for ClO_4^-. Anal. Calc. for $C_{49}H_{40.5}N_8O_{15.25}Cl_2Cu_2$: C, 49.73; H, 3.45; N, 9.47. Found: C, 49.81; H, 2.98; N, 9.32%.

$\{[Cu(phen)_2]_2(\mu_2\text{-}CO_3)\}(ClO_4)_2\cdot DMF\cdot H_2O$ (4). The powder crystals (**3**) mentioned above were recrystallized from DMF through diethyl ether diffusion and blue-green crystals were isolated after a few days, suitable for X-ray analysis. IR ν/cm^{-1} (KBr pressed pellet): 1665s and 1364s for CO_3^{2-}, 1087s for ClO_4^-. Anal. Calc. for $C_{52}H_{41}N_9O_{13}Cl_2Cu_2$: C, 52.14; H, 3.45; N, 10.52. Found: C, 52.05; H, 3.48; N, 10.35%.

$[(bpy)_2(H_2O)Zn(\mu_2\text{-}CO_3)Zn(bpy)_2](NO_3)_2\cdot 7H_2O$ (5). To a solution containing 0.288 g (1.0 mmol) of $Zn(NO_3)_2\cdot 3H_2O$ and 0.312 g (2.0 mmol) of bpy in 20 mL of water, 0.336 g (4.0 mmol) of $NaHCO_3$ was added. The solution was filtered and allowed to stand in air for slow evaporation. After a few days, 0.322 g (60.4%) of yellow block crystals were obtained, suitable for X-ray analysis. IR ν/cm^{-1} (KBr pressed pellet): 1636m and 1354s for CO_3^{2-}, 1766w and 1382s for NO_3^-. Anal. Calc. for $C_{41}H_{48}N_{10}O_{17}Zn_2$: C, 45.44; H, 4.46; N, 12.93. Found: C, 46.26; H, 4.68; N, 13.03%.

Physical measurements

Infrared spectra were recorded on a Nicolet 5SX instrument using the KBr pellet method. UV-Vis absorption spectra were recorded on a Shimadzu UV-2101PC scanning spectrophotometer using a tandem cuvette at 25 °C. The spectra of $[Cu(bpy)_2(H_2O)](NO_3)_2$ and $[Cu(phen)_2(H_2O)](NO_3)_2$ were recorded in the absence and presence of 0.10 M $NaHCO_3$ as a function of pH. The absorbance at 340 nm as a function of pH is shown for both complexes in Fig. 1. ^{13}C NMR measurements on the Zn(II) complex were performed on a Bruker DPX 300 MHz spectrometer. Magnetic measurements were carried out on polycrystalline samples with a SQUID apparatus working in the range 5–300 K under a magnetic field of 10000 G. Diamagnetic corrections were estimated from a Pascal table.

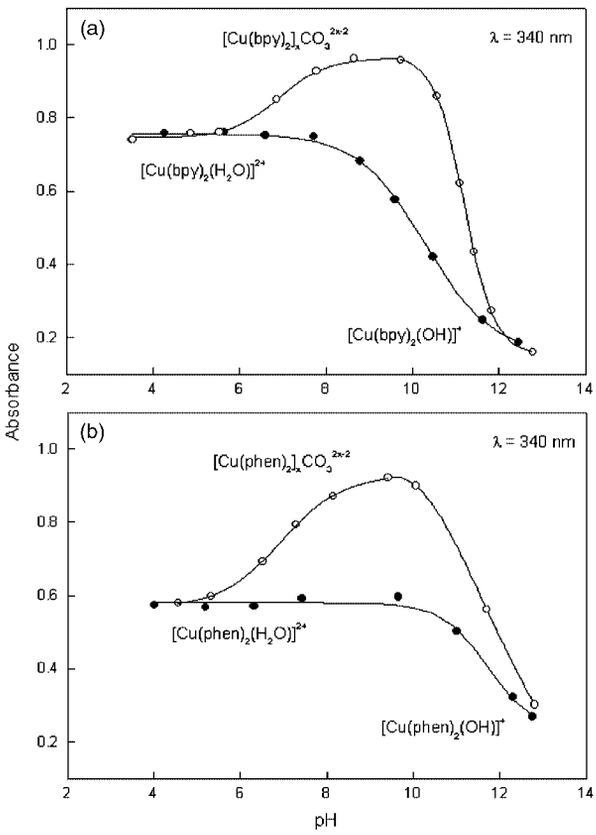

Fig. 1 Visible absorption spectra of (a) 1.25 mM $[Cu(bpy)_2(H_2O)]^{2+}$ and (b) 0.625 mM $[Cu(phen)_2(H_2O)]^{2+}$ as a function of pH in the absence (●) and presence (○) of 0.10 M HCO_3^- at $T = 25.0 \pm 0.1$ °C and ionic strength = 0.25 M ($NaNO_3$).

X-Ray structure analysis

Analyses of the isolated crystals **1** to **5** were carried out on Siemens P4 (**1**, **2**, **3**, and **5**) and Philips PW1100/10 (**4**) diffractometers with graphite monochromated Mo-Kα radiation. Intensity data were collected using either ω-scans (**1**, **2**, **3**, and **5**) or the $\omega/2\theta$-scan technique (**4**) and corrected for Lorentz and polarization effects. A semiempirical absorption correction using Psi-scans was carried out for **2**, **3**, and **5**, while absorption effects in **1** were corrected using ΔF^2 methods.[26] Structures were solved by direct methods using SHELXTL 5.03[27] (**1**, **2**, **3**, and **5**) and SHELXS-86[28] (**4**), respectively. All structures were refined by full-matrix least-squares methods on F^2 using SHELXTL 5.03[27] (**1**, **2**, **3**, and **5**) or SHELXTL 5.1[29] (**4**). For **1**, **2**, and **4** hydrogen atom positions were located from a difference Fourier map and refined with a fixed common isotropic U; the positional parameters of the solvate water H-atoms of **2** and of the solvate DMF H-atoms of **4** were not refined. For **3** and **5**, all hydrogen atoms are geometrically positioned with an isotropic U being 1.2 or 1.5 times the equivalent isotropic U_{eq} of the corresponding carrier atom. No H-atoms were included for the

Table 1 Crystallographic details for complexes **1**–**5**

	1	**2**	**3**	**4**	**5**
Empirical formula	$C_{25}H_{30}N_4O_{10}Cu$	$C_{25}H_{38}N_4O_{14}Cu$	$C_{49}H_{40.5}N_8Cl_2O_{15.25}Cu_2$	$C_{52}H_{41}N_9Cl_2O_{13}Cu_2$	$C_{41}H_{48}N_{10}O_{17}Zn_2$
Formula weight	610.07	682.13	1183.37	1197.95	1083.63
T/K	200(2)	295(2)	295(2)	293(2)	295(2)
λ/Å	0.71073	0.71073	0.71073	0.7093	0.71073
Space group	$P2_1/c$	$P\bar{1}$	$P\bar{1}$	$P2_1/c$	$P2_1$
a/Å	9.901(1)	11.007(2)	12.488(1)	11.44(1)	10.976(2)
b/Å	26.277(3)	11.683(2)	12.832(1)	21.57(1)	14.009(2)
c/Å	10.510(3)	13.345(2)	30.367(4)	20.26(1)	16.347(3)
α/°	90	78.18(1)	90.05(1)	90	90
β/°	105.93(2)	75.83(2)	91.93(1)	91.4(1)	107.84(1)
γ/°	90	70.37(3)	94.78(1)	90	90
V/Å^3	2629.4(9)	1553.0(5)	4846.5(8)	4998(6)	2392.7(7)
Z	4	2	4	4	2
ρ(calc.)/Mg m^{-3}	1.541	1.459	1.622	1.592	1.504
μ(MoKα)/mm^{-1}	0.896	0.776	1.069	1.036	1.084
T_{min}/T_{max}	0.053/0.175	0.484/0.518	0.527/0.681	—	0.310/0.360
F(000)	1268	714	2418	2448	1120
Crystal size/mm	0.80 × 0.60 × 0.40	0.62 × 0.58 × 0.45	0.38 × 0.22 × 0.15	0.73 × 0.33 × 0.28	0.50 × 0.45 × 0.40
θ range/°	2.14–27.00	1.87–27.01	1.79–25.00	2.59–24.95	1.95–27.00
hkl ranges	−13/12, 0/34, 0/13	−13/1, −14/14, −17/16	−1/14, −15/15, −36/36	0/13, −25/25, −24/24	−1/14, −17/1, −20/20
Reflections collected	7033	7840	19647	17510	6784
Independent reflections	5739	6759	17065	8772	5872
R(int)	0.1726	0.0113	0.0465	0.0519	0.0391
Observed refl. [$I > 2\sigma(I)$]	4355	5545	7307	5826	3551
Goodness-of-fit on F^2	1.016	1.075	1.031	1.051	1.052
R_1[a] [$I > 2\sigma(I)$]	0.0533	0.0447	0.0882	0.0453	0.0606
wR_2[b] (all data)	0.1413	0.1219	0.2367	0.1188	0.1508
Largest diff. peak/e Å^{-3}	0.606, −1.454	0.481, −0.381	0.507, −0.556	0.688, −0.482	0.344, −0.712

[a] $R_1 = \Sigma||F_o| - |F_c||/\Sigma|F_o|$. [b] $wR_2 = [\Sigma w(F_o^2 - F_c^2)/\Sigma wF_o^2)^2]^{1/2}$.

solvate water molecules in **3**. Crystallographic data and data collection parameters are summarized in Table 1, and selected bond distances and bond angles are given in Tables 2 to 6. Labelled diagrams of complexes **1** to **5** are shown in Fig. 2 to 6, respectively.

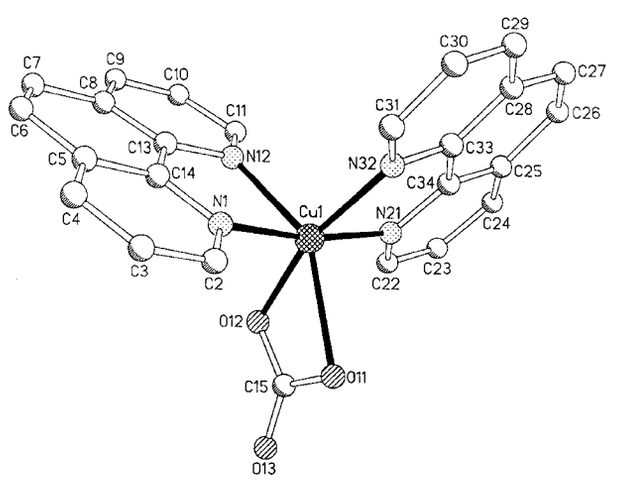

Fig. 2 Molecular structure of $[Cu(phen)_2(CO_3)]$ (**1**).

CCDC reference numbers 164327–164331.

See http://www.rsc.org/suppdata/dt/b1/b103942n/ for crystallographic data in CIF or other electronic format.

Kinetic measurements

Complex solutions were prepared freshly with ultrapure water shortly before the kinetic measurements. The HCO_3^- solutions were prepared by dissolving $NaHCO_3$ crystals, 0.20 M HNO_3 was added slowly to adjust the pH to the appropriate value, and the solutions were used within 5 h.[11] Kinetic measurements were performed at 25.0 ± 0.1 °C on a Biologic SFM-3 stopped-flow instrument, and monitored with an attached on-line data acquisition and handling system. One syringe was filled with the $[Cu(bpy)_2(H_2O)]^{2+}/HCO_3^-$ solution (pH = 6.0) and the other syringe with 0.25 M CAPS buffer solution (pH = 10.0). The complex-formation reaction was studied as a function of $[Cu(bpy)_2(H_2O)^{2+}]$, $[Cu(phen)_2(H_2O)^{2+}]$ and $[HCO_3^-]$, respectively. The ionic strength was adjusted to 0.25 M with $NaNO_3$. The absorbance–time traces were recorded and fitted to a single exponential using the OLIS KINFIT (Bogart, Ga) set of programs. Temperature and pressure dependences were also

Table 2 Selected bond lengths (Å) and angles (°) for $[Cu(phen)_2(CO_3)]\cdot 7H_2O$ (**1**)

Cu(1)–O(12)	1.972(3)	Cu(1)–N(21)	2.030(3)
Cu(1)–N(1)	2.034(3)	Cu(1)–N(32)	2.071(3)
Cu(1)–N(12)	2.243(3)	Cu(1)–O(11)	2.421(3)
C(15)–O(13)	1.252(4)	C(15)–O(11)	1.272(4)
C(15)–O(12)	1.313(4)		
O(12)–Cu(1)–N(21)	92.7(1)	O(12)–Cu(1)–N(1)	94.4(1)
N(21)–Cu(1)–N(1)	170.8(1)	O(12)–Cu(1)–N(32)	164.8(1)
N(21)–Cu(1)–N(32)	80.6(1)	N(1)–Cu(1)–N(32)	94.0(1)
O(12)–Cu(1)–N(12)	88.98(9)	N(21)–Cu(1)–N(12)	95.4(1)
N(1)–Cu(1)–N(12)	78.8(1)	N(32)–Cu(1)–N(12)	105.1(1)
O(12)–Cu(1)–O(11)	58.47(9)	N(21)–Cu(1)–O(11)	96.5(1)
N(1)–Cu(1)–O(11)	92.2(1)	N(32)–Cu(1)–O(11)	108.5(1)
N(12)–Cu(1)–O(11)	145.72(9)	O(13)–C(15)–O(11)	125.2(3)
O(13)–C(15)–O(12)	119.6(3)	O(11)–C(15)–O(12)	115.1(3)

Table 3 Selected bond lengths (Å) and angles (°) for $[Cu(phen)_2(CO_3)]\cdot 11H_2O$ (**2**)

Cu(1)–O(12)	1.964(2)	Cu(1)–N(21)	2.010(2)
Cu(1)–N(1)	2.021(2)	Cu(1)–N(32)	2.056(2)
Cu(1)–N(12)	2.250(2)	C(15)–O(11)	1.262(4)
C(15)–O(13)	1.264(3)	C(15)–O(12)	1.300(3)
O(12)–Cu(1)–N(21)	93.27(8)	O(12)–Cu(1)–N(1)	94.22(8)
N(21)–Cu(1)–N(1)	172.50(8)	O(12)–Cu(1)–N(32)	171.43(8)
N(21)–Cu(1)–N(32)	81.18(9)	N(1)–Cu(1)–N(32)	91.33(8)
O(12)–Cu(1)–N(12)	94.50(8)	N(21)–Cu(1)–N(12)	101.15(8)
N(1)–Cu(1)–N(12)	78.80(8)	N(32)–Cu(1)–N(12)	92.99(8)
O(11)–C(15)–O(13)	123.6(3)	O(11)–C(15)–O(12)	116.4(2)
O(13)–C(15)–O(12)	120.0(3)		

Table 4 Selected bond lengths (Å) and angles (°) for $\{[Cu(phen)_2]_2(\mu_2\text{-}CO_3)\}(ClO_4)_2\cdot 4.25H_2O$ (**3**)

Cu(1)–O(11)	1.951(6)	Cu(1)–N(21)	2.020(8)
Cu(1)–N(1)	2.027(7)	Cu(1)–N(32)	2.033(8)
Cu(1)–N(12)	2.241(7)	Cu(2)–O(12)	1.925(6)
Cu(2)–N(72)	2.016(7)	Cu(2)–N(61)	2.029(7)
Cu(2)–N(41)	2.047(7)	Cu(2)–N(52)	2.263(8)
O(11)–C(15)	1.300(10)	O(12)–C(15)	1.317(11)
O(13)–C(15)	1.241(11)	Cu(3)–N(81)	1.994(10)
Cu(3)–N(101)	1.999(10)	Cu(3)–N(92)	2.131(10)
Cu(3)–N(112)	2.156(10)	Cu(3)–O(22)	2.30(2)
Cu(4)–N(152)	2.010(9)	Cu(4)–N(132)	2.030(9)
Cu(4)–N(141)	2.130(8)	Cu(4)–N(121)	2.164(9)
Cu(4)–O(21)	2.192(14)	O(21)–C(95)	1.260(14)
O(22)–C(95)	1.21(2)	O(23)–C(95)	1.23(2)
O(11)–Cu(1)–N(21)	91.1(3)	O(11)–Cu(1)–N(1)	94.7(3)
N(21)–Cu(1)–N(1)	170.7(3)	O(11)–Cu(1)–N(32)	161.4(3)
N(21)–Cu(1)–N(32)	81.5(3)	N(1)–Cu(1)–N(32)	95.0(3)
O(11)–Cu(1)–N(12)	97.6(3)	N(21)–Cu(1)–N(12)	93.8(3)
N(1)–Cu(1)–N(12)	78.3(3)	N(32)–Cu(1)–N(12)	99.8(3)
O(12)–Cu(2)–N(72)	93.2(3)	O(12)–Cu(2)–N(61)	174.0(3)
N(72)–Cu(2)–N(61)	80.7(3)	O(12)–Cu(2)–N(41)	90.6(3)
N(72)–Cu(2)–N(41)	174.5(3)	N(61)–Cu(2)–N(41)	95.4(3)
O(12)–Cu(2)–N(52)	92.3(3)	N(72)–Cu(2)–N(52)	104.9(3)
N(61)–Cu(2)–N(52)	89.2(3)	N(41)–Cu(2)–N(52)	78.8(3)
O(13)–C(15)–O(11)	122.3(10)	O(13)–C(15)–O(12)	123.2(9)
O(11)–C(15)–O(12)	114.5(9)	N(81)–Cu(3)–N(101)	171.0(4)
N(81)–Cu(3)–N(92)	80.3(4)	N(101)–Cu(3)–N(92)	90.7(4)
N(81)–Cu(3)–N(112)	100.1(4)	N(101)–Cu(3)–N(112)	80.0(4)
N(92)–Cu(3)–N(112)	96.1(3)	N(81)–Cu(3)–O(22)	97.7(4)
N(101)–Cu(3)–O(22)	88.8(4)	N(92)–Cu(3)–O(22)	131.0(4)
N(112)–Cu(3)–O(22)	131.8(4)	N(152)–Cu(4)–N(132)	173.2(4)
N(152)–Cu(4)–N(141)	79.8(3)	N(132)–Cu(4)–N(141)	93.5(4)
N(152)–Cu(4)–N(121)	99.1(4)	N(132)–Cu(4)–N(121)	79.9(4)
N(141)–Cu(4)–N(121)	93.1(3)	N(152)–Cu(4)–O(21)	94.6(3)
N(132)–Cu(4)–O(21)	92.2(4)	N(141)–Cu(4)–O(21)	166.2(3)
N(121)–Cu(4)–O(21)	100.2(3)	O(22)–C(95)–O(23)	124(2)
O(22)–C(95)–O(21)	119(2)	O(23)–C(95)–O(21)	117(2)

Table 5 Selected bond lengths (Å) and angles (°) for $\{[Cu(phen)_2]_2(\mu_2\text{-}CO_3)\}(ClO_4)_2\cdot DMF\cdot H_2O$ (**4**)

Cu(1)–O(11)	1.933(3)	Cu(1)–N(1)	2.013(4)
Cu(1)–N(21)	2.039(3)	Cu(1)–N(12)	2.045(4)
Cu(1)–N(32)	2.215(4)	Cu(2)–O(12)	1.938(3)
Cu(2)–N(61)	2.029(4)	Cu(2)–N(72)	2.030(4)
Cu(2)–N(52)	2.036(4)	Cu(2)–N(41)	2.258(4)
O(11)–C(15)	1.307(5)	O(12)–C(15)	1.305(5)
O(13)–C(15)	1.253(5)		
O(11)–Cu(1)–N(1)	93.5(2)	O(11)–Cu(1)–N(21)	93.2(1)
O(11)–Cu(1)–N(32)	90.7(2)	O(11)–Cu(1)–N(12)	174.0(2)
N(1)–Cu(1)–N(21)	164.0(2)	N(1)–Cu(1)–N(12)	81.5(2)
N(1)–Cu(1)–N(32)	115.5(2)	N(12)–Cu(1)–N(21)	90.8(2)
N(12)–Cu(1)–N(32)	94.6(2)	N(21)–Cu(1)–N(32)	78.9(2)
O(12)–Cu(2)–N(41)	105.6(2)	O(12)–Cu(2)–N(52)	91.0(2)
O(12)–Cu(2)–N(61)	162.2(2)	O(12)–Cu(2)–N(72)	91.2(2)
N(41)–Cu(2)–N(52)	78.0(2)	N(41)–Cu(2)–N(61)	91.6(2)
N(41)–Cu(2)–N(72)	99.0(2)	N(52)–Cu(2)–N(61)	97.3(2)
N(52)–Cu(2)–N(72)	176.7(2)	N(61)–Cu(2)–N(72)	81.2(2)
O(11)–C(15)–O(12)	115.5(4)	O(11)–C(15)–O(13)	121.8(4)
O(12)–C(15)–O(13)	122.7(4)		

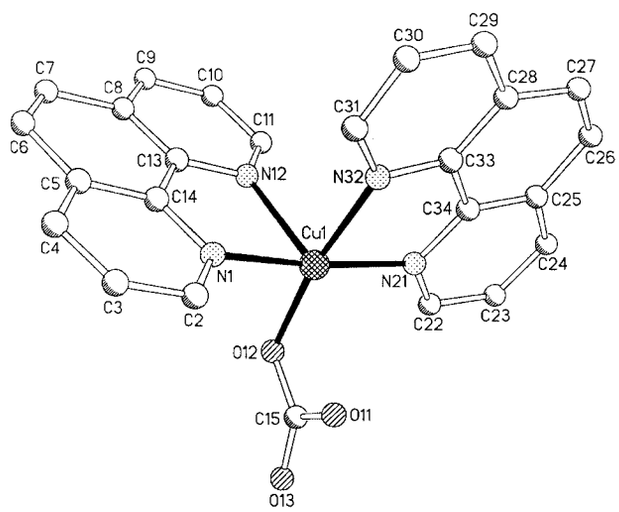

Fig. 3 Molecular structure of $[Cu(phen)_2(CO_3)]$ (**2**).

studied. The pH values of all solutions were measured immediately before and after the reactions using a Metrohm 632 pH meter equipped with an Ingold V402-S7/120 electrode.

Results and discussion

UV-Vis spectra

It is seen from Fig. 1(a) that interesting spectral changes occur in the metal-to-ligand charge transfer band. In the absence of HCO_3^-, the absorbance at 340 nm undergoes a sigmoid change over the pH range 8 to 12, which can be ascribed to deprotonation of the coordinated water molecule in $[Cu(bpy)_2(H_2O)]^{2+}$. The conditional pK_a value of 10.3 ± 0.1 is given by the inflection of the sigmoid curve. Similar spectral changes are observed for $[Cu(phen)_2(H_2O)]^{2+}$ in the pH range 10 to 13 (see Fig. 1(b)), and the corresponding pK_a value of 11.7 ± 0.3 was directly obtained. In the presence of HCO_3^-, the absorbance increases from pH 6 to a maximum at pH 10, and then abruptly decreases on increasing the pH further to 12.5. These spectral changes can be assigned to the substitution of coordinated H_2O by HCO_3^-, and the subsequent substitution of coordinated carbonate by OH^-. In the first process, the coordinated water in $[Cu(bpy)_2(H_2O)]^{2+}$ and $[Cu(phen)_2(H_2O)]^{2+}$ is substituted by HCO_3^- and carbonato complexes are gradually formed. An apparent pK_a value of *ca.* 7.0 ± 0.1 is obtained from Fig. 1, which lies within the range of values reported for other bicarbonato metal complexes ($[ML_n(OCO_2H)]$).[1i] When the pH is

Table 6 Selected bond lengths (Å) and angles (°) for complex $[(bpy)_2(H_2O)Zn(\mu_2\text{-}CO_3)Zn(bpy)_2](NO_3)_2\cdot 7H_2O$ (**5**)

Zn(1)–O(12)	2.048(7)	Zn(1)–O(11)	2.119(7)
Zn(1)–N(22)	2.149(7)	Zn(1)–N(11)	2.152(7)
Zn(1)–N(12)	2.155(9)	Zn(1)–N(21)	2.176(9)
O(12)–C(1)	1.261(11)	C(1)–O(21)	1.310(11)
C(1)–O(22)	1.309(10)	C(1)–Zn(2)	2.542(10)
Zn(2)–O(21)	2.116(7)	Zn(2)–N(32)	2.125(9)
Zn(2)–N(41)	2.132(8)	Zn(2)–N(42)	2.145(7)
Zn(2)–N(31)	2.149(8)	Zn(2)–O(22)	2.172(7)
O(12)–Zn(1)–O(11)	91.7(3)	O(12)–Zn(1)–N(22)	91.4(3)
O(11)–Zn(1)–N(22)	88.9(3)	O(12)–Zn(1)–N(11)	95.0(3)
O(11)–Zn(1)–N(11)	95.7(3)	N(22)–Zn(1)–N(11)	172.0(4)
O(12)–Zn(1)–N(12)	91.2(3)	O(11)–Zn(1)–N(12)	170.6(3)
N(22)–Zn(1)–N(12)	99.9(3)	N(11)–Zn(1)–N(12)	75.2(3)
O(12)–Zn(1)–N(21)	167.9(3)	O(11)–Zn(1)–N(21)	89.0(3)
N(22)–Zn(1)–N(21)	76.5(3)	N(11)–Zn(1)–N(21)	97.0(3)
N(12)–Zn(1)–N(21)	90.1(3)	C(1)–O(12)–Zn(1)	130.1(7)
O(12)–C(1)–O(21)	120.6(9)	O(12)–C(1)–O(22)	124.4(10)
O(21)–C(1)–O(22)	114.9(9)	O(12)–C(1)–Zn(2)	174.0(7)
O(21)–C(1)–Zn(2)	56.2(5)	O(22)–C(1)–Zn(2)	58.7(5)
O(21)–Zn(2)–N(32)	160.1(3)	O(21)–Zn(2)–N(41)	100.2(3)
N(32)–Zn(2)–N(41)	97.1(3)	O(21)–Zn(2)–N(42)	93.7(3)
N(32)–Zn(2)–N(42)	99.6(4)	N(41)–Zn(2)–N(42)	77.5(3)
O(21)–Zn(2)–N(31)	90.1(3)	N(32)–Zn(2)–N(31)	77.7(4)
N(41)–Zn(2)–N(31)	98.3(3)	N(42)–Zn(2)–N(31)	174.8(5)
O(21)–Zn(2)–O(22)	62.0(2)	N(32)–Zn(2)–O(22)	102.6(3)
N(41)–Zn(2)–O(22)	159.1(3)	N(42)–Zn(2)–O(22)	92.2(3)
N(31)–Zn(2)–O(22)	92.7(3)	O(21)–Zn(2)–C(1)	31.0(3)
N(32)–Zn(2)–C(1)	132.3(3)	N(41)–Zn(2)–C(1)	130.5(3)
N(42)–Zn(2)–C(1)	94.1(4)	N(31)–Zn(2)–C(1)	91.0(3)
O(22)–Zn(2)–C(1)	31.0(2)		

higher than 10, coordinated carbonate is displaced by OH^- due to an increase in $[OH^-]$. When the pH is less than 6, complex species mainly exist in the form of $[Cu(bpy)_2(H_2O)]^{2+}$ and $[Cu(phen)_2(H_2O)]^{2+}$.

^{13}C NMR spectra

Due to the low solubility of complex **5** in water, ^{13}C NMR spectra were recorded in a 1 : 1 mixture of D_2O–DMSO-d_6. ^{13}C labelling to form $[(bpy)_2(H_2O)Zn(\mu_2\text{-}^{13}CO_3)Zn(bpy)_2](NO_3)_2\cdot 7H_2O$ revealed a weak multiple peak at 166.9–168.3 ppm for the μ_2-CO_3 group, a strong peak at 161.5 ppm for free HCO_3^- and a strong peak at 126.5 ppm for free CO_2. The chemical shift for the μ_2-CO_3 group carbon atom lies within the range reported for other carbonato complexes of Zn(II).[20h,20i,30] The $[Cu(bpy)_2(H_2O)]^{2+}$ complex is expected to exhibit a similar behavior in the presence of bicarbonate.

Structures

Before the crystal structures of five carbonato complexes are described in more detail below, attention is first given to some general aspects concerning these structures.

Chirality. All five compounds are chiral. The two monomeric complexes **1** and **2** form racemates and both enantiomers are present within the crystal structure. The stereochemical description is *OC*-6–22-*C* for the *Λ*-isomer (shown in Fig. 2 and 3) and *OC*-6–22-*A* for the corresponding *Δ*-isomer (not shown). For the dinuclear complexes **3**, **4** and **5**, the formation of diastereomers has to be considered and the situation is significantly more complex. The observed molecular structures reveal the formation of heterochiral *Λ*,*Δ*-isomers in all three cases (shown in Fig. 4, 5 and 6). Whereas **3** and **4** again form racemates, spontaneous resolution occurred in the case of **5** and the studied crystal contained only one enantiomer of the *Λ*,*Δ*-isomer.

Pseudo-Jahn–Teller behavior. The Cu(II) compounds **1**, **2**, **3** and **4** represent pseudo-Jahn–Teller systems showing a typical distortion of the octahedral coordination mode. In their molecular structures the mean Cu–N axial bond lengths (Cu1–N12, Cu1–N32) are significantly (by 0.11 to 0.14 Å) shorter than the Cu–N equatorial bond distances (Cu1–N1, Cu1–N21). The Cu–O bond distances vary over a wide range from 1.925(6) and 3.066(8) Å to 2.30(2) and 2.44(2) Å depending on the carbonate binding mode. Within this variation, there is a systematic pattern of distortion from C_2 symmetry of the carbonate ligand: (i) as one Cu–O bond lengthens, the other shortens; (ii) as a Cu–O bond lengthens (shortens), the Cu–N bond *trans* to it also lengthens (shortens). This is in line with observations made for a series of $[ML_2(OXO)]Y$ complexes (M = Cu, Zn; L = phen, bpy; X = N, C; Y = BF_4, PF_6, ClO_4, NO_3).[31,32] A significant change can also be observed in the anisotropic displacement parameters of the O atoms of coordinated carbonate depending on the coordination mode. The O atom Gaussian ellipsoids are small and nearly isotropic when carbonate coordinates in a very asymmetric way, whereas they get large and very anisotropic for the symmetrical coordination mode.[32] By way of example, the equatorial atoms in molecule 1 (around Cu1) and 2 (around Cu3) are shown in Fig. 7.

Carbonate coordination modes. The objective of this study was to focus on the different coordination modes of carbonate in the studied complexes. The most important structural features can be summarized as follows:

*$[Cu(phen)_2(CO_3)]\cdot 7H_2O$ (**1**).* Fig. 2 shows that the N_4-coordinated Cu(II) ion is coordinated by carbonate in a way between the limiting monodentate or bidentate modes: the bond lengths for Cu1–O11 and Cu1–O12 are 2.421(3) and 1.972(3) Å, respectively. The bond angle of N32–Cu1–N12 is 105.09(10)° (see Table 2), which means that the coordination polyhedron of the copper atom is between a distorted tetragonal pyramidal and an octahedral arrangement. An approximate plane consists of the N12, N32, and Cu1 atoms and the carbonate group, the maximum deviation from a least-squares plane calculated through these 8 atoms amounts to 0.199(2) Å for O11. Three water molecules can be found in the vicinity of the carbonate and form hydrogen bridges (O11 ··· O1 2.668(4), O12 ··· O5[$x-1, y, z$] 2.703(4), O13 ··· O1[$-x+2, -y, -z+1$] 2.662(4) and O13 ··· O3[$x-1, y, z$] 2.647(4) Å).

*$[Cu(phen)_2(CO_3)]\cdot 11H_2O$ (**2**).* The structure of complex **2** is similar to that of complex **1**, but has stronger monodentate distortion. The bond lengths for Cu1–O11 and Cu1–O12 are 2.556(2) and 1.964(2) Å, respectively (see Fig. 3). The bond angle of N32–Cu1–N12 is 92.99(8)° (see Table 3), which means that the coordination polyhedron of the copper atom can be described with a tetragonal pyramidal assignment with N12 occupying the apical position. The carbonate coordinates to the copper atom along the base plane. The angle between two least-squares planes calculated through the atoms of the carbonate group and the base plane of the tetragonal pyramid, respectively, amounts to 88.41(9)°. At least five water molecules exist around the carbonate ion and form hydrogen bridges (O11 ··· O21 2.686(3), O12 ··· O22 2.763(3), O13 ··· O23 2.804(4), O13 ··· O25 2.836(4) and O13 ··· O26 2.836(4) Å).

In general, the carbonate ion has a higher basicity than the bicarbonate ion and thus, in a monomeric system, it is suggested that it has a stronger tendency to coordinate to Cu(II) in a bidentate mode.[8b] However, the large number of water molecules around the carbonate ion in the monomeric complex most likely prevents the carbonate ion from binding to Cu(II) in a bidentate mode, due to the resulting hydrogen bonding network. A comparison of the O11–Cu1 distance and the number of surrounding water molecules in both complexes indicates that this effect is more obvious for the complex with the larger number of water molecules. By way of comparison, the X-ray structures of two bicarbonato complexes of bis(phenanthroline)copper(II) were recently resolved.[16d] In $[Cu(phen)_2O_2COH]ClO_4$, bicarbonate is coordinated in a bidentate mode with

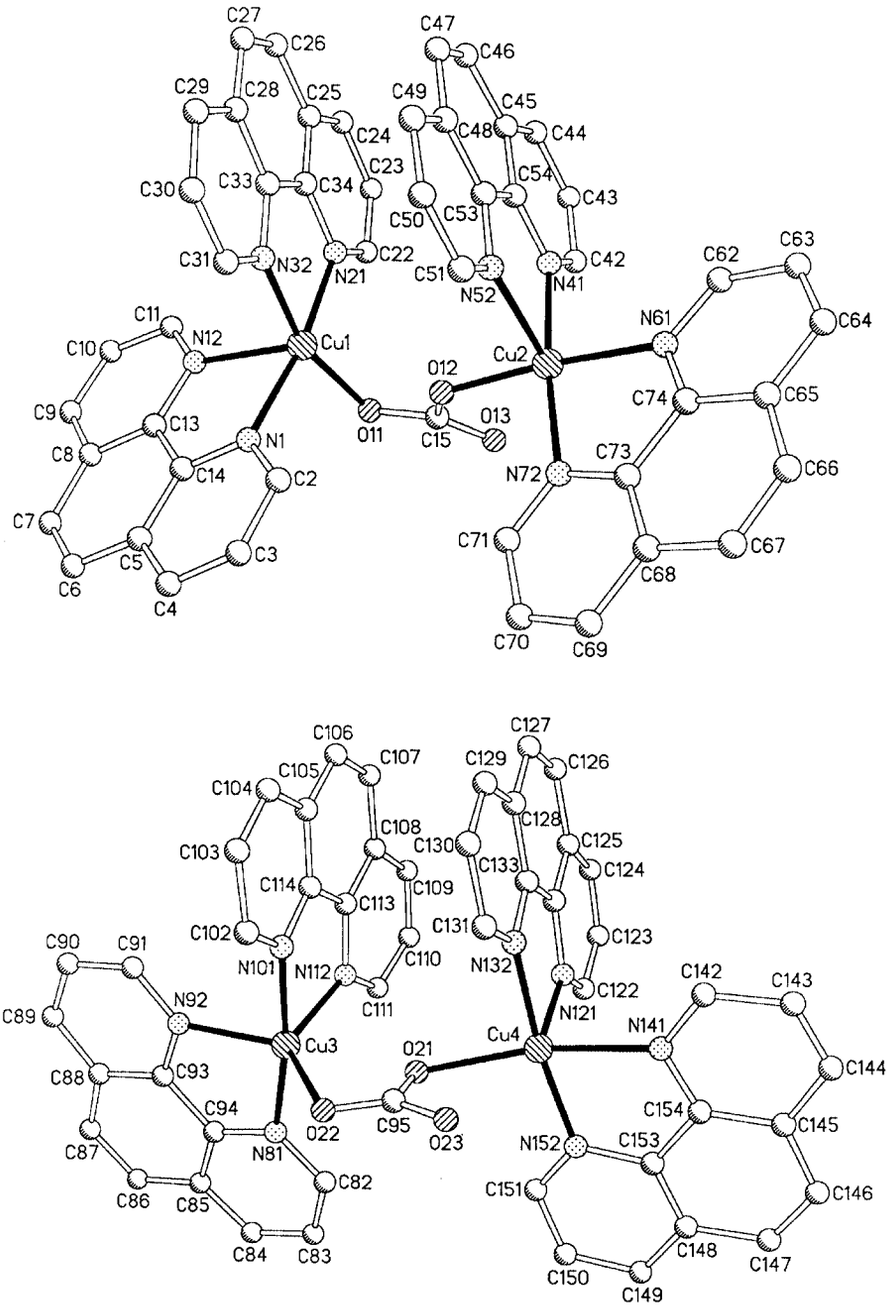

Fig. 4 Molecular structure of $\{[Cu(phen)_2]_2(\mu_2\text{-}CO_3)\}^{2+}$ (**3**).

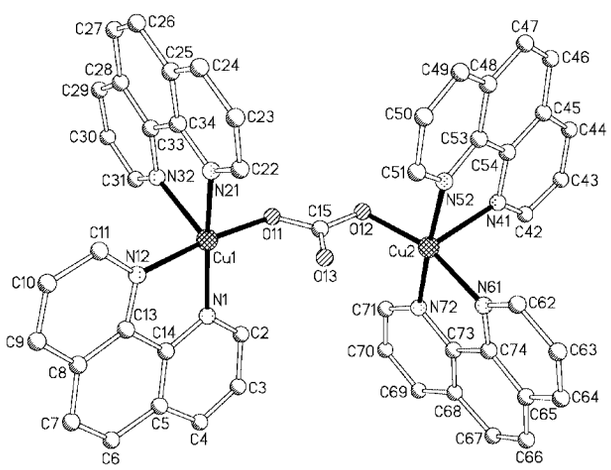

Fig. 5 Molecular structure of $\{[Cu(phen)_2]_2(\mu_2\text{-}CO_3)\}^{2+}$ (**4**).

two equal Cu–O distances of 2.359 Å, whereas in $[Cu(phen)_2OCO_2H]ClO_4$ bicarbonate is coordinated in a monodentate mode with Cu–O distances of 1.998 and 3.045 Å, respectively. The Cu–O bond lengths quoted for complexes **1** and **2** above, differ significantly from these values. Protonation of the weaker bound end of the carbonate ligand clearly leads to a significant lengthening of this bond from 2.421 and 2.556 in **1** and **2**, respectively, to 3.045 Å in $[Cu(phen)_2OCO_2H]ClO_4$. The other Cu–O bond is hardly affected by this protonation and remains almost constant in all three structures. Protonation of the carbonyl function of the carbonate ligand leads to a highly symmetric bicarbonato complex, $[Cu(phen)_2O_2COH]ClO_4$, in which both Cu–O bond lengths are identical.[16d]

*$\{[Cu(phen)_2]_2(\mu_2\text{-}CO_3)\}(ClO_4)_2\cdot 4.25H_2O$ (**3**).* In the crystals there are two molecular units of identical composition but distinct structures (see Fig. 4). In molecule 1 (Fig. 4, upper), the bond distances for Cu1–O11, Cu1–O12, Cu2–O12 and Cu2–O13 are 1.951(6), 2.565(6), 1.925(6) and 3.066(6) Å, respectively

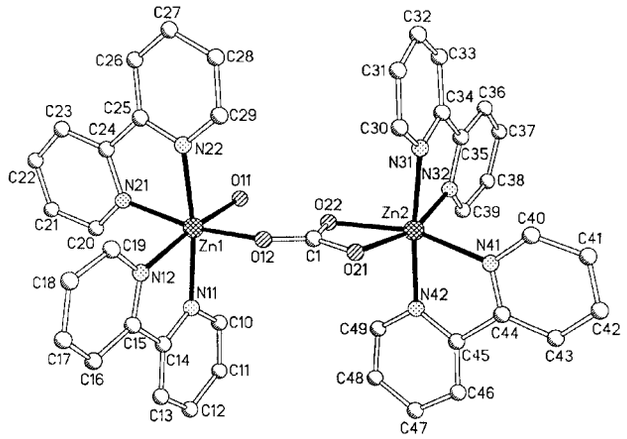

Fig. 6 Molecular structure of $[(bpy)_2(H_2O)Zn(\mu_2\text{-}CO_3)Zn(bpy)_2]^{2+}$ (**5**).

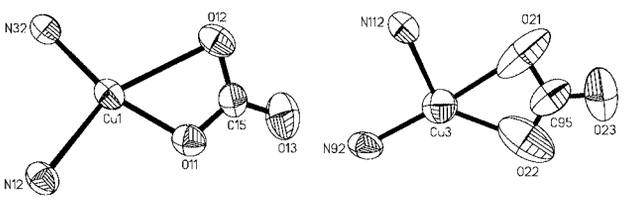

Fig. 7 ORTEP drawing (50% probability ellipsoids) of the equatorial atoms in molecule 1 (around Cu1, left) and molecule 2 (around Cu3, right) of complex **3**.

(see Table 4). These structural data indicate that the two N_4-coordinated Cu(1) and Cu(2) ions are bridged by carbonate approximately bidentately and monodentately, respectively. In carbonate-bridged binuclear metal systems, there are only six possible theoretical structures and they are listed in Scheme 2.

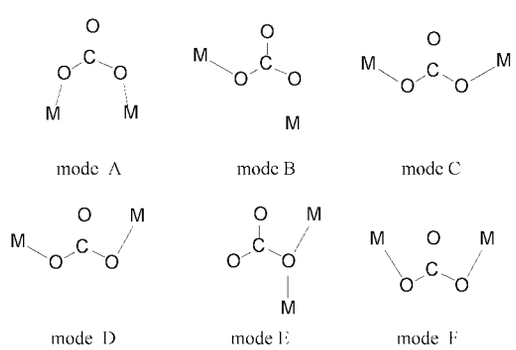

Scheme 2 Summary of typical carbonate coordination modes in binuclear systems.

Molecule 1 in complex **3** shows a distortion between modes B and E, and approaches mode E, which is the mode not reported so far. The coordination polyhedron of the two copper atoms can be described with a tetragonal pyramidal structure. The carbonate coordinates to two copper atoms along the base planes. In molecule 2 (Fig. 4, lower) the bond distances for Cu3–O22 and Cu3–O21 are 2.30(2) and 2.44(2) Å, respectively and the bond distances for Cu4–O21 and Cu4–O23 are 2.19(2) and 2.44(2) Å, respectively (see Table 4). Both the N_4-coordinated Cu(II) ions are bridged by carbonate in approximately a bidentate way to form a binuclear complex, and the carbonate coordination mode can approximately be described by mode F. The coordination polyhedron of the two copper atoms show a distorted trigonal bipyramidal structure for Cu3 and a distorted tetragonal pyramidal structure for Cu4. The carbonate ion coordinates to two copper atoms in the plane positions. The distances of Cu1 ··· Cu2 in molecule 1 and Cu3 ··· Cu4 in molecule 2 are 4.303(2) and 4.548(2) Å, respectively. The phen ligands show strong stacking effects in the crystal.

{[Cu(phen)$_2$]$_2$(μ_2-CO$_3$)}(ClO$_4$)$_2$·DMF·H$_2$O (**4**). The structure is different from the two forms in complex **3**, but similar to the reported structure of $\{[Cu(bpy)_2]_2(\mu_2\text{-}CO_3)\}(ClO_4)_2$.[20d] It is seen from Fig. 5 that the two N_4-coordinated Cu(II) ions are bridged by carbonate in monodentate and *anti–anti* modes to form a binuclear complex. The bond distances for Cu1–O11 and Cu1–O13 are 1.933(3) and 2.844(4) Å, respectively and the bond distances for Cu2–O12 and Cu2–O13 are 1.938(3) and 2.693(4) Å, respectively (see Table 5). The coordination polyhedron of the two copper atoms can be described with an approximately tetragonal pyramidal geometry. The distance of Cu1 ··· Cu2 is 5.296(5) Å. The carbonate coordinates to two copper atoms along the base planes.

[(bpy)$_2$(H$_2$O)Zn(μ_2-CO$_3$)Zn(bpy)$_2$](NO$_3$)$_2$·7H$_2$O (**5**). Fig. 6 shows a labelled diagram for complex **5**. See Table 6 for selected bond lengths and angles. The two N_4-coordinated Zn1 and Zn2 ions are bridged by carbonate in monodentate and bidentate modes, respectively, to form a binuclear complex. The Zn1 atom is coordinated to one water molecule. The coordination polyhedron of the two zinc atoms can be described as an octahedron, but the environment of Zn2 is strongly distorted due to the coordination to the carbonate bridge. The short O11–O22 distance of 2.610(10) Å indicates that there is one H-bond between CO_3^{2-} and the H_2O molecule, thereby forming a six-membered ring. The distance of Zn1 ··· Zn2 is 5.400(1) Å. An approximate least-squares plane consists of N21, N12, Zn1, O11, O12, C1, O22, O21, Zn2, N32 and N41, from which the Zn1 and Zn2 atoms deviate by 0.0262(3) and 0.0293(3) Å, respectively. The structure of another related μ_3-carbonate product has been reported.[20c]

The above-mentioned four carbonate binuclear complexes exhibit different bridging modes, shown in Scheme 2. In the bidentate mode, an unexpected behavior is that the bond lengths between Zn and the oxygen atoms of the carbonate ligand are shorter than the bond lengths between Cu and the oxygen atoms of carbonate.

Magnetism

Variable-temperature magnetic susceptibility measurements were performed on powdered samples in the range 5–300 K. The magnetic behavior of complexes **3** and **4** is shown in Fig. 8(a) and 8(b), respectively, in the form of χ_m *vs.* T and $\chi_m T$ *vs.* T plots. It is seen that both the values of $\chi_m T$ increase slowly with decreasing temperature from 300 K to 5 K on account of an increased population of an $S = 1$ ground state. This indicates the existence of weak ferromagnetic coupling in both these complexes. The coupling most likely occurs in an intramolecular fashion between two carbonate-bridged Cu(II) ions rather than by intermolecular interactions to neighbouring molecules.

Over the whole temperature range of 5–300 K, the magnetic data of both complexes very closely follow the theoretical expression of the magnetic susceptibility for a copper(II) pair:

$$\chi_m = \frac{2N\beta^2 g^2}{kT}[3 + \exp(-J/kT)]^{-1}(1-\rho) + \frac{N\beta^2 g^2}{2kT}\rho + 0.000120$$

in which the second term accounts for a small proportion ρ of uncoupled copper(II). J is the singlet–triplet (S–T) energy gap, and the other parameters have their usual meaning. The minimization of

$$R = \Sigma\,(\chi_m^{calc} - \chi_m^{obs})^2/\Sigma(\chi_m^{obs})^2$$

leads to the following parameters:

$J = 13.0$ cm^{-1} $g = 2.00$ $\rho = 0.01$ $R = 0.00034$ for complex **3**

$J = 0.013$ cm^{-1} $g = 2.21$ $\rho = 0.001$ $R = 0.00054$ for complex **4**

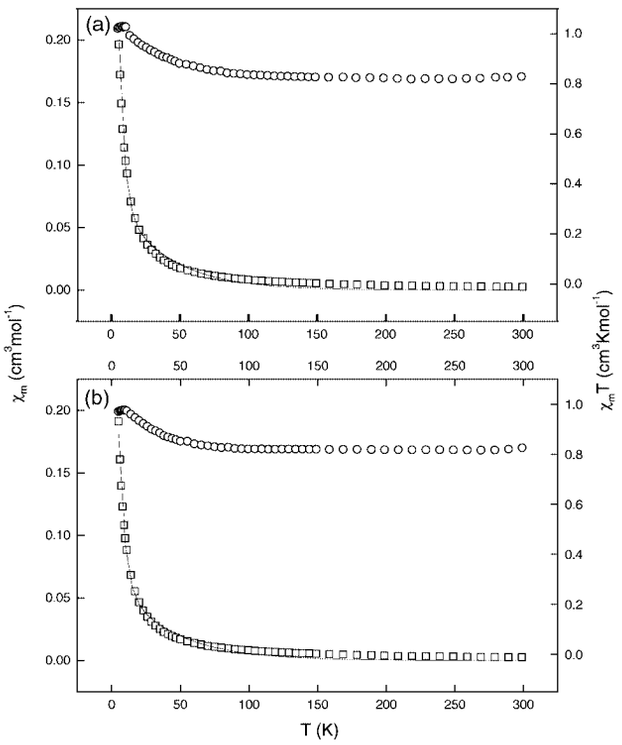

Fig. 8 Plots of χ_m *vs.* T (□) and $\chi_m T$ *vs.* T (○) for (a) complex **3** and (b) complex **4**. The best calculated fit is given as a solid line.

The difference in J for both complexes no doubt reflects the difference in the Cu–Cu distance and the simultaneous effect of the carbonate-bridging mode. In complex **3** the J value should be an average produced by both carbonate-bridging modes. These results are also similar to those reported earlier,[19g,k] which show the presence of weak intramolecular ferromagnetic coupling.

Kinetics

The kinetics of the reaction of $[Cu(bpy)_2(H_2O)]^{2+}$ and $[Cu(phen)_2(H_2O)]^{2+}$ with HCO_3^- was studied using stopped-flow and T-jump techniques. On mixing two syringes, one filled with a HCO_3^- solution and the other with a buffered solution of $[Cu(bpy)_2(H_2O)]^{2+}$ or $[Cu(phen)_2(H_2O)]^{2+}$, in the stopped-flow instrument, no kinetic traces could be observed over the entire pH range of 6 to 10, although a significant spectral change did occur on mixing these solutions in a tandem cuvette. Furthermore, the reaction could also not be observed using the T-jump technique on mixtures of these solutions under the selected conditions. In view of the relatively high pK_a values of $[Cu(bpy)_2(H_2O)]^{2+}$ and $[Cu(phen)_2(H_2O)]^{2+}$, and the low pK_a value of carbonic acid, the reactions between $[Cu(bpy)_2(OH)]^+$ or $[Cu(phen)_2(OH)]^+$ and CO_2 are probably not important in the selected pH range. The results, therefore, indicate that the substitution of coordinated H_2O by HCO_3^- and CO_3^{2-} in $[Cu(bpy)_2(H_2O)]^{2+}$ and $[Cu(phen)_2(H_2O)]^{2+}$ must be very fast on the stopped-flow/T-jump time-scale, which is in good agreement with the substitution data reported for $[Cu(tren)(H_2O)]^{2+}$.[20i,33] A clear kinetic trace could only be observed on the stopped-flow instrument using a pH-jump technique in which one syringe was filled with a mixture of $[Cu(bpy)_2(H_2O)]^{2+}$ or $[Cu(phen)_2(H_2O)]^{2+}$ and HCO_3^- (pH *ca.* 6) and the other syringe filled with a buffer solution (pH *ca.* 10). The resulting kinetic trace exhibited good first-order behavior, and k_{obs} could be measured as a function of complex and HCO_3^- concentration. From the results shown in Fig. 9, it follows that k_{obs} is independent of the selected concentrations which implies that all reactions between HCO_3^- and $[Cu(bpy)_2(H_2O)]^{2+}$ or $[Cu(phen)_2(H_2O)]^{2+}$ must be non-rate-determining steps.

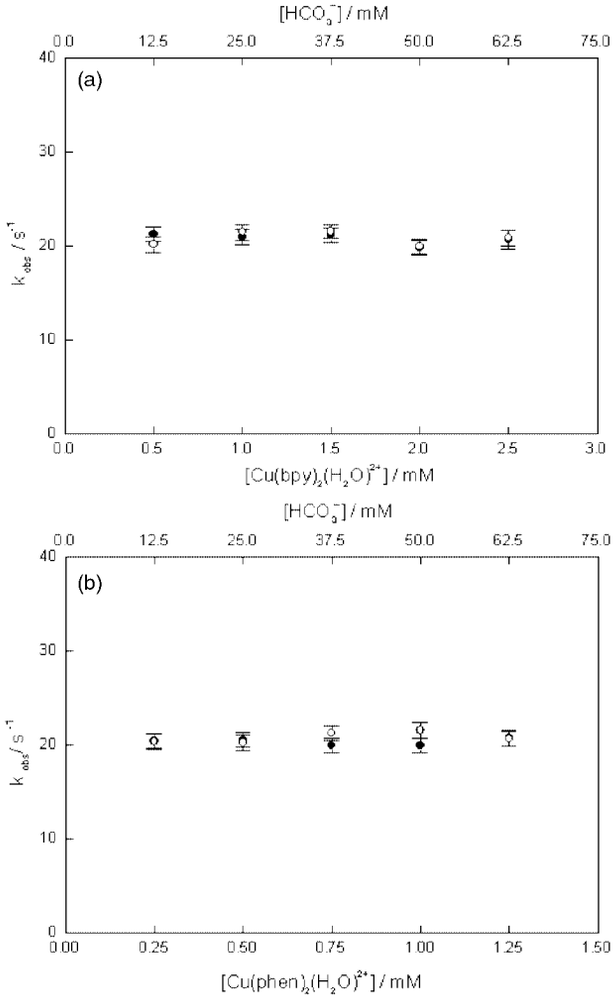

Fig. 9 Plot of (a) k_{obs} *vs.* $[Cu(bpy)_2(H_2O)^{2+}]$ (●) at 50 mM HCO_3^-, and k_{obs} *vs.* $[HCO_3^-]$ (○) at 1.0 mM $[Cu(bpy)_2(H_2O)]^{2+}$; (b) k_{obs} *vs.* $[Cu(phen)_2(H_2O)^{2+}]$ (●) at 50 mM HCO_3^-, and k_{obs} *vs.* $[HCO_3^-]$ (○) at 0.5 mM $[Cu(phen)_2(H_2O)]^{2+}$. T = 25.0 ± 0.1 °C and ionic strength = 0.25 M ($NaNO_3$).

Due to the high lability of coordinated H_2O in $[Cu(bpy)_2(H_2O)]^{2+}$ and $[Cu(phen)_2(H_2O)]^{2+}$, substitution by HCO_3^- is expected to occur in a rapid equilibration. In general, monomeric bicarbonato complexes are unstable, especially in the case of a monodentate structure, and undergo reverse aquation or decarboxylation. Since no kinetic traces were observed on mixing $[Cu(bpy)_2(H_2O)]^{2+}$ or $[Cu(phen)_2(H_2O)]^{2+}$ and buffer in the absence of HCO_3^-, the concentration independent kinetics observed in the presence of bicarbonate must correspond to a change in the binding mode of the unstable bicarbonato intermediate, presumably from a five-coordinate monodentate to a pseudo-six-coordinate bidentate or a related mode. Thus during the pH-jump, the bicarbonato complex is deprotonated, followed by the rate-determining ring-closure of $[Cu(bpy)_2OCO_2]$ to $[Cu(bpy)_2O_2CO]$, or $[Cu(phen)_2OCO_2]$ to $[Cu(phen)_2O_2CO]$, in order to account for the concentration independence of the observed kinetics. The rate-determining step can be formulated as in eqn. (2), for which k_{obs} has an average value of 20.7 ± 0.8 s^{-1} at 25 °C, estimated from the data in Fig. 9. This step is then followed by the subsequent partial formation of binuclear carbonato bridged species as suggested in eqn. (3), on the basis of the structural data reported in this paper. The reaction sequence can be summarized as follows (L = bpy or phen):

$$[Cu(L)_2(H_2O)]^{2+} + HCO_3^- \rightleftharpoons [Cu(L)_2OCO_2H]^+ + H_2O, \text{ fast} \quad (1)$$

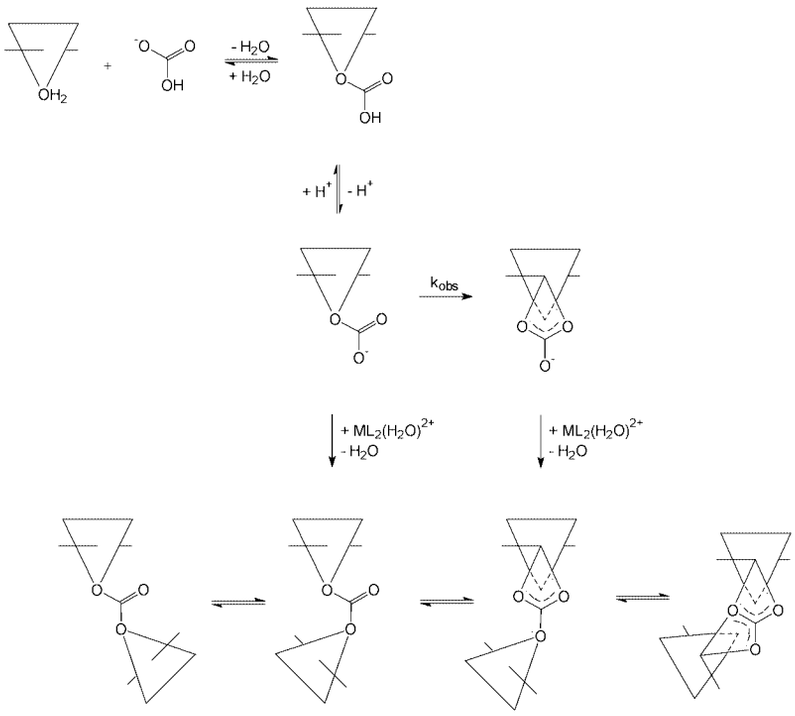

Scheme 3 Proposed mechanism for carbonation of CuN_4 with a planar water molecule in the trigonal bipyramidal structure.

$$[Cu(L)_2OCO_2H]^+ \text{ (5-coord.)} \longrightarrow [Cu(L)_2O_2CO] \text{ (6-coord.)} + H^+,\ k_{obs} \quad (2)$$

$$[Cu(L)_2O_2CO] + [Cu(L)_2(H_2O)]^{2+} \rightleftharpoons \{[Cu(L)_2]_2(\mu\text{-}CO_3)\}^{2+} + H_2O \quad (3)$$

Eqn. (1) represents the rapid complex-formation step that occurs during mixing of the aqua complex with bicarbonate. Eqn. (2) is suggested to account for the pH-jump induced kinetic trace and to involve ring-closure of the unstable five-coordinate bicarbonato complex to produce the pseudo-octahedral six-coordinate carbonato complex as described above.

In an effort to obtain more information on the nature of the rate-determining step induced by the pH-jump, the temperature and pressure dependences of this reaction were studied (see ref. 34 for details on the high pressure stopped-flow instrument employed), and the results are presented in Fig. 10 and 11,

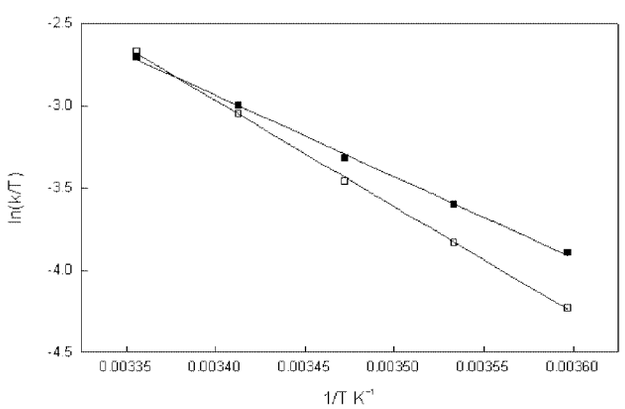

Fig. 10 Temperature dependence of k_{obs} for the reaction of 1.0 mM $[Cu(bpy)_2(H_2O)]^{2+}$ (■) and 0.5 mM $[Cu(phen)_2(H_2O)]^{2+}$ (□) with 50 mM HCO_3^- and ionic strength = 0.25 M ($NaNO_3$).

respectively. The thermal and pressure activation parameters are summarized in Table 7. It follows from the significantly negative $\Delta S^{\#}$ and $\Delta V^{\#}$ values that eqn. (2) involves bond formation and/or an increase in electrostriction.[35] Ring-closure

Table 7 Kinetic parameters for the reaction of $[Cu(bpy)_2(H_2O)]^{2+}$ and $[Cu(phen)_2(H_2O)]^{2+}$ with HCO_3^-

Parameter	$[Cu(bpy)_2(H_2O)]^{2+}$	$[Cu(phen)_2(H_2O)]^{2+}$
pK_a	≥10.3 ± 0.1	≥11.7 ± 0.3
k/s^{-1}, 25 °C	20.7 ± 0.8	20.5 ± 0.8
$\Delta H^{\#}$/kJ mol^{-1}	41.2 ± 0.9	53.7 ± 0.8
$\Delta S^{\#}$/J mol^{-1} K^{-1}	−82.0 ± 2.5	−39.6 ± 2.5
$\Delta G^{\#}$/kJ mol^{-1}, 25 °C	65.7 ± 0.9	65.5 ± 0.8
$\Delta V^{\#}$/cm^3 mol^{-1}, 15 °C	−16.9 ± 0.4	−26.6 ± 1.0

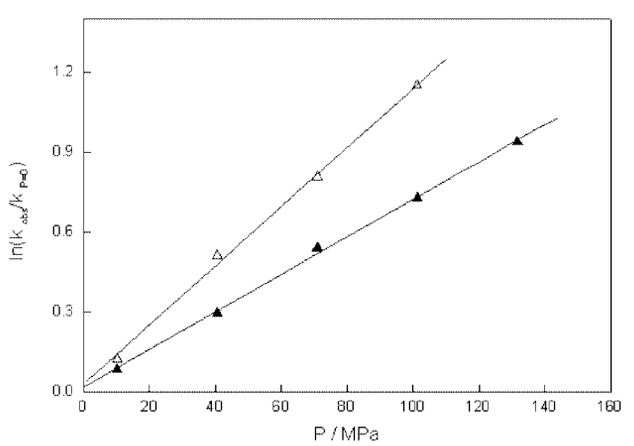

Fig. 11 Pressure dependence of k_{obs} for the reaction of 1.0 mM $[Cu(bpy)_2(H_2O)]^{2+}$ (▲) and 0.5 mM $[Cu(phen)_2(H_2O)]^{2+}$ (△) with 50 mM HCO_3^-. T = 15.0 ± 0.1 °C and ionic strength = 0.25 M ($NaNO_3$).

reactions are in general accompanied by a significant decrease in partial molar volume. In addition, the release of a proton results in a significant increase in electrostriction and will also contribute to a volume collapse. Thus an overall negative volume of activation is in line with the suggested rate-determining reaction (2).

An overall plausible mechanism for the carbonation reaction of $[Cu(bpy)_2(H_2O)]^{2+}$ and $[Cu(phen)_2(H_2O)]^{2+}$ with HCO_3^- (eqn. (1)) is proposed in Scheme 3. Complex-formation of $[Cu(L)_2(H_2O)]^{2+}$ with HCO_3^- is a rapid process and produces

the monodentate bicarbonato species at low pH. With increasing pH, carbonation is enhanced in that the monodentate bicarbonato intermediate forms a pseudo-bidentate species which is accompanied by deprotonation of coordinated bicarbonate. The pseudo-bidentate intermediate is suggested to be a deprotonated complex as shown in eqn. (2), which subsequently produces a series of complexes of the type $\{[Cu(L)_2]_2(\mu_2\text{-}CO_3)\}^{2+}$ in eqn. (3). The CO_2 uptake reaction route does not compete efficiently due to the high pK_a value of $[Cu(L)_2(H_2O)]^{2+}$, *i.e.* due to the low fraction of hydroxo complex ions present in solution.

Conclusions

The kinetic study of the reaction of $[Cu(bpy)_2(H_2O)]^{2+}$ and $[Cu(phen)_2(H_2O)]^{2+}$ with HCO_3^- indicates that the five-coordinate copper complex with distorted trigonal bipyramidal structure is active towards substitution of H_2O by HCO_3^- when H_2O is located in the in-plane position. The reaction is so fast that it could not be studied by stopped-flow and T-jump techniques. The unstable monodentate bicarbonato intermediate produces a carbonato complex in a kinetically observable step. No catalytic activity of this complex is expected on the basis of the formation of bicarbonato and carbonato complexes that do not undergo a decarboxylation reaction. CO_2 uptake by the investigated $[CuL_2(H_2O)]^{2+}$ complexes is prevented by the relatively high pK_a values of the aqua complexes, which results in the formation of $[CuL_2OH]^+$ in a pH range where too little CO_2 is present in solution. Thus in the present case the carbonation process contributes significantly to the overall observed reaction, an aspect that may be important to consider in studies on the catalytic activity of model complexes.

Acknowledgements

We gratefully acknowledge financial support from the Deutsche Forschungsgemeinschaft and the Fonds der Chemischen Industrie, and the award of a fellowship by the Alexander von Humboldt Foundation and financial support by the National Natural Science Foundation of China to Z.-W. M. We wish to thank Professor D. Sellmann for generous support of this work.

References

1 (*a*) E. Kimura, *Acc. Chem. Res.*, 2001, **34**, 171; (*b*) W. N. Lipscomb and N. Strater, *Chem. Rev.*, 1996, **96**, 2375; (*c*) K. Hakansson, A. Svensson and A. Lijas, *J. Mol. Biol.*, 1992, **227**, 1192; (*d*) S. J. Dodgson, R. E. Tashian, G. Gros and N. D. Carter, *The Carbonic Anhydrases*, Plenum Press, New York, 1991; (*e*) D. W. Christianson, *Adv. Protein Chem.*, 1991, **41**, 281; (*f*) F. Botre, G. Gros and B. T. Storey, *Carbonic Anhydrase*, VCH, Weinhein, Germany, 1991; (*g*) D. N. Silverman and S. Lindskog, *Acc. Chem. Res.*, 1988, **21**, 30; (*h*) J. E. Coleman, in *Zinc Enzymes*, ed. I. Bertini, C. Luchinat, W. Maret and M. Zeppezauer, Birkhäuser, Boston, MA, 1986, p. 317; (*i*) D. A. Palmer and R. van Eldik, *Chem. Rev.*, 1983, **83**, 51; (*j*) I. Bertini, C. Luchinat and A. Scozzafava, *Struct. Bonding*, 1982, **48**, 45; (*k*) H. Steiner, B. H. Jonsson and S. Lindskog, *Eur. J. Biochem.*, 1975, **59**, 253.

2 (*a*) M. Hartmann, K. M. Merz Jr., R. van Eldik and T. Clark, *J. Mol. Model.*, 1998, **4**, 355; (*b*) M. Hartmann, T. Clark and R. van Eldik, *J. Am. Chem. Soc.*, 1997, **119**, 7843; (*c*) K. M. Merz Jr. and L. Banci, *J. Am. Chem. Soc.*, 1997, **119**, 863; (*d*) M. Sola, A. Ledos, M. Duran and J. Betran, *J. Am. Chem. Soc.*, 1992, **114**, 869; (*e*) Y.-J. Zheng and K. M. Merz, *J. Am. Chem. Soc.*, 1992, **114**, 10498; (*f*) D. R. Garmer and M. Krauss, *J. Am. Chem. Soc.*, 1992, **114**, 6487; (*g*) K. M. Merz Jr., R. Hoffmann and M. J. S. Dewar, *J. Am. Chem. Soc.*, 1989, **111**, 5636; (*h*) R. Rowlett and D. N. Silverman, *J. Am. Chem. Soc.*, 1982, **104**, 6737.

3 (*a*) K. K. Kannan, M. Petef, H. Cid-Dresdner and S. Lövgren, *FEBS Lett.*, 1977, **73**, 115; (*b*) K. K. Kannan, B. Noststrand, K. Fridborg, S. Lövgren, A. Ohlessen and M. Petef, *Proc. Natl. Acad. Sci. USA.*, 1975, **72**, 51; (*c*) A. Liljas, K. K. Kannan, P. C. Bergsten, I. Waara, K. Fridborg, B. Strandberg, U. Carlbom, L. Jarup, S. Lovgren and M. Petef, *Nature (London), New Biol.*, 1972, **235**, 131; (*d*) K. K. Kannan, A. Liljas, I. Waara, P. C. Bergsten, S. Lovgren, B. Strandberg, U. Bengtsson, U. Carlbom and K. Fridborg, *Cold Spring Harbour Symp. Quant. Biol.*, 1971, **36**, 221; (*e*) Y. Xue, J. Vidgren, L. A. Svensson, A. Liljas, B.-H. Jonsson and S. Lindskog, *Proteins*, 1993, **15**, 80; (*f*) V. Kumar and K. K. Kannan, *J. Mol. Biol.*, 1994, **241**, 226.

4 (*a*) I. Tabushi, Y. Kuroda and A. Mochizuki, *J. Am. Chem. Soc.*, 1980, **102**, 1152; (*b*) J. M. Harrowfield, V. Norris and A. M. Sargeson, *J. Am. Chem. Soc.*, 1976, **98**, 7282; (*c*) P. Woolley, *Nature*, 1975, **258**, 677.

5 (*a*) M. L. M. Pennings, D. N. Reinhoudt, S. Harkema and G. J. van Hummel, *J. Am. Chem. Soc.*, 1980, **102**, 7571; (*b*) R. Menif, J. Reibenspies and A. E. Martell, *Inorg. Chem.*, 1991, **30**, 3446; (*c*) F. Meyer and P. Rutsch, *Chem. Commun.*, 1998, 1037.

6 (*a*) R. S. Brown, N. J. Curtis and J. Huguet, *J. Am. Chem. Soc.*, 1981, **103**, 6953; (*b*) R. S. Brown, D. Salmon, N. J. Curtis and S. Kusuma, *J. Am. Chem. Soc.*, 1982, **104**, 3188; (*c*) H. Slebocka-Tilk, J. L. Cocho, Z. Frakman and R. S. Brown, *J. Am. Chem. Soc.*, 1984, **106**, 2421.

7 (*a*) T. Koike, E. Kimura, I. Nakamura, Y. Hashimoto and M. Shiro, *J. Am. Chem. Soc.*, 1992, **114**, 7338; (*b*) T. Koike and E. Kimura, *J. Am. Chem. Soc.*, 1991, **113**, 8935; (*c*) E. Kimura, T. Shiota, T. Koike, M. Shiro and M. Kodama, *J. Am. Chem. Soc.*, 1990, **112**, 5805.

8 (*a*) M. Kimblin, W. E. Allen and G. Parkin, *J. Chem. Soc., Chem. Commun.*, 1995, 1813; (*b*) A. Looney and G. Parkin, *Inorg. Chem.*, 1994, **33**, 1234; (*c*) A. Looney, R. Han, K. MeNeill and G. Parkin, *J. Am. Chem. Soc.*, 1993, **115**, 4690.

9 (*a*) R. Alsfasser, M. Ruf, S. Trofimenko and H. Vahrenkamp, *Chem. Ber.*, 1993, **126**, 685; (*b*) R. Alsfasser, S. Trofimenko, A. Looney, G. Parkin and H. Vahrenkamp, *Inorg. Chem.*, 1991, **30**, 4098.

10 N. Kitajima, S. Hikichi, M. Tanaka and Y. Moro-oka, *J. Am. Chem. Soc.*, 1993, **115**, 5496.

11 X. Zhang, C. D. Hubbard and R. van Eldik, *J. Phys. Chem.*, 1996, **100**, 9161.

12 (*a*) X. Zhang and R. van Eldik, *Inorg. Chem.*, 1995, **34**, 5606; (*b*) X. Zhang, R. van Eldik, T. Koike and E. Kimura, *Inorg. Chem.*, 1993, **32**, 5749.

13 T. Itoh, Y. Fujii, T. Tada, Y. Yoshikawa and H. Hisada, *Bull. Chem. Soc. Jpn.*, 1996, **69**, 1265.

14 L. Cronin, B. Greener, S. P. Foxon, S. L. Heath and P. H. Walton, *Inorg. Chem.*, 1997, **36**, 2594.

15 C. Bazzicalupi, A. Bencini, A. Bianchi, F. Corana, V. Fusi, P. Giorgi, P. Paoli, P. Paoletti, B. Valtancoli and C. Zanchini, *Inorg. Chem.*, 1996, **35**, 5540.

16 (*a*) T. Yoshida, D. L. Thorn, T. Okano, J. A. Ibers and S. Otsuka, *J. Am. Chem. Soc.*, 1979, **101**, 4212; (*b*) D. J. Darensbourg, M. L. M. Jones and J. H. Reibenspies, *Inorg. Chem.*, 1993, **32**, 4675; (*c*) K. E. Baxter, L. R. Hanton, J. Simpson, B. R. Vincent and A. G. Blackman, *Inorg. Chem.*, 1995, **34**, 2795; (*d*) Z.-W. Mao, G. Liehr and R. van Eldik, *J. Am. Chem. Soc.*, 2000, **122**, 4839.

17 (*a*) R. Menif, J. Reibenspies and A. E. Martell, *Inorg. Chem.*, 1991, **30**, 3446; (*b*) F. Meyer and P. Rutsch, *Chem. Commun.*, 1998, 1037.

18 T. Tanase, S. Nitta, S. Yoshikawa, K. Kobayashi, T. Sakural and S. Yano, *Inorg. Chem.*, 1992, **31**, 1058.

19 (*a*) T. Yoshida, W. J. Youngs, T. Sakaeda, T. Ueda, S. Otsuka and J. A. Ibers, *J. Am. Chem. Soc.*, 1983, **105**, 6273; (*b*) E. G. Lundquist, K. Folting, J. C. Huffman and K. G. Caulton, *Inorg. Chem.*, 1987, **26**, 205; (*c*) J. Sletten, H. Hope, M. Julve, O. Kahn, M. Verdaguer and A. Dworkin, *Inorg. Chem.*, 1988, **27**, 542; (*d*) H. Harada, M. Kodera, G. Vuckovic, N. Matsumoto and S. Kida, *Inorg. Chem.*, 1991, **30**, 1190; (*e*) L. Spiccia, G. D. Fallon, A. Markiewicz, K. S. Murray and H. Riesen, *Inorg. Chem.*, 1992, **31**, 1066; (*f*) S. C. Rawle, C. J. Harding, P. Moore and N. W. Alcock, *J. Chem. Soc., Chem. Commun.*, 1992, 1701; (*g*) A. L. van den Brenk, K. A. Byriel, D. P. Fairlie, L. R. Gahan, G. R. Hanson, C. J. Hawkins, A. Jones, C. H. L. Kennard, B. Moubaraki and K. S. Murray, *Inorg. Chem.*, 1994, **33**, 3549; (*h*) N. Ehlers and R. Mattes, *Inorg. Chim. Acta*, 1995, **236**, 203; (*i*) C. Pariya, V. G. Puranik and N. R. Chaudhuri, *Chem. Commun.*, 1997, 1307; (*j*) A. Escuer, R. Vicente, S. B. Kumar, X. Solans and M. Font-Bardia, *J. Chem. Soc., Dalton Trans.*, 1997, 403; (*k*) A. Escuer, F. A. Mautner, E. Penalba and R. Vicente, *Inorg. Chem.*, 1998, **37**, 4190; (*l*) S. K. Mandal, D. M. Ho, G. Q. Li and M. Orchin, *Polyhedron*, 1998, **17**, 607; (*m*) J. Dietrich, F. W. Heinemann, A. Schrodt and S. Schindler, *Inorg. Chim. Acta*, 1999, **288**, 206.

20 (*a*) G. Kolks, S. J. Lippard and J. V. Waszczak, *J. Am. Chem. Soc.*, 1980, **102**, 4832; (*b*) N. N. Murthy and K. D. Karlin, *J. Chem. Soc., Chem. Commun.*, 1993, 1236; (*c*) X.-M. Chen, Q.-Y. Deng, G. Wang and Y.-J. Xu, *Polyhedron*, 1994, **13**, 3085; (*d*) P. E. Kruger, G. D. Fallon, B. Moubaraki, K. J. Berry and K. S. Murray, *Inorg. Chem.*, 1995, **33**, 4808; (*e*) A. Escuer, R. Vicente, E. Penalba, X. Solans and M. Font-Bardia, *Inorg. Chem.*, 1996, **35**, 248; (*f*) A. Escuer, R.

Vicente, S. B. Kumar, X. Solans, M. Font-Bardia and A. Caneschi, *Inorg. Chem.*, 1996, **35**, 3094; (*g*) C. Bazzicalupi, A. Bencini, A. Bianchi, F. Corana, V. Fusi, P. Giorgi, P. Paoli, P. Paoletti, B. Valtancoli and C. Zanchini, *Inorg. Chem.*, 1996, **35**, 5540; (*h*) A. Schrodt, A. Neubrand and R. van Eldik, *Inorg. Chem.*, 1997, **36**, 4579; (*i*) Z.-W. Mao, G. Liehr and R. van Eldik, *J. Chem. Soc., Dalton Trans.*, in press.
21 (*a*) F. W. B. Einstein and A. C. Willis, *Inorg. Chem.*, 1981, **20**, 609; (*b*) R. Alvarez, J. L. Atwood, E. Carmona, P. J. Perez, M. L. Poveda and R. D. Rogers, *Inorg. Chem.*, 1991, **30**, 1493; (*c*) G. B. Deacon, T. Feng, D. C. R. Hockless, P. C. Junk, B. W. Skelton and A. H. White, *Chem. Commun.*, 1997, 341; (*d*) A. Escuer, E. Penalba, R. Vicente, X. Solans and M. Font-Bardia, *J. Chem. Soc., Dalton Trans.*, 1997, 2315.
22 T. C. W. Mak, P.-J. Li, C.-M. Chen and K.-Y. Huang, *J. Chem. Soc., Chem. Commun.*, 1986, 1597.
23 P. D. Brotherton and A. H. White, *J. Chem. Soc., Dalton Trans.*, 1973, 2338.
24 W. D. Harrison and B. J. Hathaway, *Acta Crystallogr., Sect. B*, 1979, **35**, 2910.
25 H. Nakai and Y. Deguchi, *Bull. Chem. Soc. Jpn.*, 1975, **48**, 2557.
26 S. Parkin, B. Moezzi and H. Hope, *J. Appl. Crystallogr.*, 1995, **28**, 53.
27 SHELXTL 5.03 for Siemens Crystallographic Research Systems, 1995, Siemens Analytical X-ray Instruments Inc., Madison, WI, USA.
28 G. M. Sheldrick, *Acta Crystallogr., Sect. A*, 1990, **46**, 467.
29 SHELXTL NT 5.1, 1998, Bruker AXS, Inc., Madison, WI, USA.
30 M. Kato and T. Ito, *Inorg. Chem.*, 1985, **24**, 504.
31 C. J. Simmons, B. J. Hathaway, K. Amornjarusiri, B. D. Santasiero and A. Clearfield, *J. Am. Chem. Soc.*, 1987, **109**, 1947.
32 C. J. Simmons, *New J. Chem.*, 1993, **17**, 77.
33 D. H. Powell, A. E. Merbach, L. Fabian, S. Schindler and R. van Eldik, *Inorg. Chem.*, 1994, **33**, 4468.
34 R. van Eldik, W. Gaede, S. Wieland, J. Kraft, M. Spitzer and D. A. Palmer, *Rev. Sci. Instrum.*, 1993, **64**, 1355.
35 (*a*) R. van Eldik, T. Asano and W. J. le Noble, *Chem. Rev.*, 1989, **89**, 549; (*b*) A. Drljaca, C. D. Hubbard, R. van Eldik, T. Asano, M. V. Basilevsky and W. J. le Noble, *Chem. Rev.*, 1998, **98**, 2167.